



Testing DDE and Constraining high- z reionization with Cosmological Data

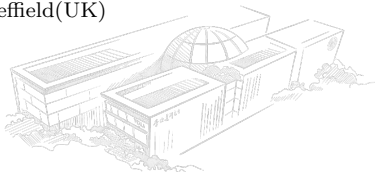
arXiv: 2505.02932, 2506.19096

Speaker: Hanyu Cheng

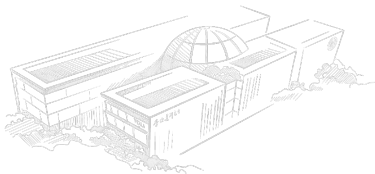
chenghanyu@sjtu.edu.cn

Tsung-Dao Lee Institute(China) & The University of Sheffield(UK)

June 25, 2025



- 1 **Constraining Pressure-Based Dynamical Dark Energy(DDE) Models with Latest Cosmological Data**
- 2 **Constraining exotic high- z reionization histories with Gaussian processes and the cosmic microwave background**



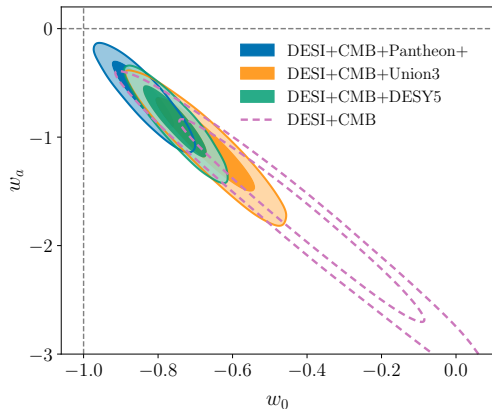
CPL Parametrization:

$$w(a) = w_0 + w_a(1 - a)$$

- ▶ Taylor expansion of EoS w
- ▶ w_0 : present-day value
- ▶ w_a : time evolution
- ▶ Λ CDM: $w_0 = -1, w_a = 0$

DESI Finding:

- ▶ Deviation from Λ CDM at $> 2\sigma$
- ▶ Hints at dynamical DE
- ▶ CMB+DESI+DESY5 shows 4.2σ preference over Λ CDM



$w_0 - w_a$ plot from The DESI DR2 paper
(arxiv:2503.14738)

Alternative to CPL:

- ▶ Taylor expansion for **pressure** p , not EoS w

$$p = -p_0 + (1 - a)p_1 + (1 - a)^2 p_2 + \dots$$

- ▶ Free Parameters: $\Omega_{1,2} \equiv \frac{3}{4} \frac{p_{1,2}}{\rho_{\text{crit}}}$
- ▶ $\Omega_{\text{DE},0} = f(p_0, p_1, p_2) = 1 - \Omega_{\text{m}} - \Omega_{\text{k}} - \Omega_{\text{r}}$
- ▶ Independent consistency check

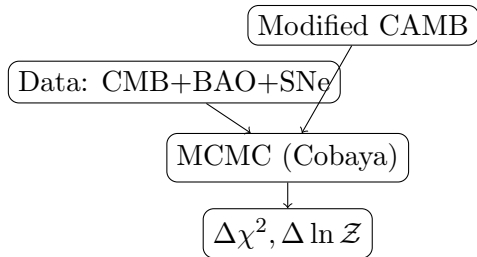
Statistical Methods:

① $\Delta\chi^2$ test:

- ▶ $\Delta\chi^2 = \chi_{\text{DDE}}^2 - \chi_{\Lambda\text{CDM}}^2$
- ▶ Convert to $N\sigma$ significance

② Bayesian Evidence:

- ▶ $\Delta \ln \mathcal{Z} = \ln \mathcal{Z}_{\text{DDE}} - \ln \mathcal{Z}_{\Lambda\text{CDM}}$
- ▶ Jeffreys' scale interpretation



Tools: CAMB, Cobaya, getdist, MCEvidence^a

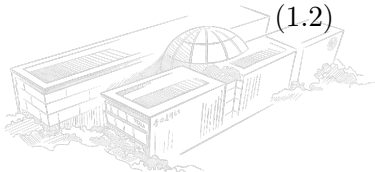
^a<https://github.com/williamgiare/wgcosmo>

The dark energy (DE) pressure can be expanded in a Taylor series around the present epoch (A. A. Sen, arXiv:0708.1072):

$$p(a) = -p_0 + \sum_{n=1}^{\infty} \frac{(1-a)^n}{n!} p_n, \quad (1.1)$$

where $-p_0$ is the current DE pressure and p_n are the higher-order coefficients. The DE density then satisfies the continuity equation:

$$\dot{\rho} + 3H(p + \rho) = 0. \quad (1.2)$$



Using the first-order term in (1.1), the DE energy density evolves as:

$$\rho(a) = \rho_{\text{DE},0} - \frac{3}{4}(1-a)p_1, \quad (1.3)$$

where $\rho_{\text{DE},0}$ is the present DE density and p_1 is the first-order pressure coefficient. Defining the dimensionless parameters

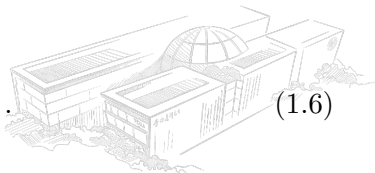
$$\Omega_{\text{DE},0} \equiv \frac{\rho_{\text{DE},0}}{\rho_{\text{crit}}}, \quad \Omega_1 \equiv \frac{3}{4} \frac{p_1}{\rho_{\text{crit}}}, \quad \rho_{\text{crit}} = \frac{3H_0^2}{8\pi G}, \quad (1.4)$$

we can rewrite (1.3) as

$$\rho(a) = \rho_{\text{DE},0} \left[1 + (a-1) \frac{\Omega_1}{\Omega_{\text{DE},0}} \right]. \quad (1.5)$$

The corresponding equation-of-state parameter is

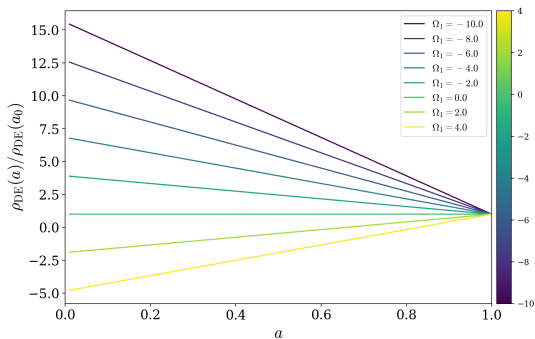
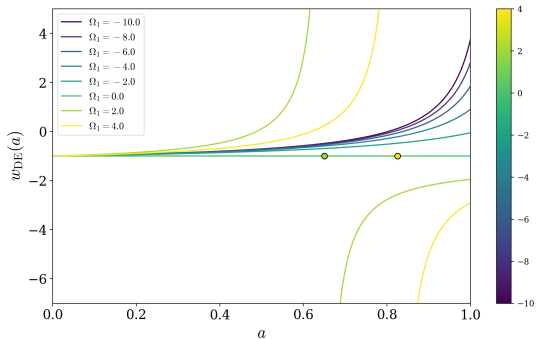
$$w_{\text{DE}}(a) = -1 + \frac{1}{3} \frac{\Omega_1 a}{\Omega_1 (1-a) - \Omega_{\text{DE},0}}. \quad (1.6)$$



Pole in the Equation of State

A singularity appears in $w_{\text{DE}}(a)$ when the denominator of (1.6) vanishes, at the scale factor

$$a_{\text{pole}} = 1 - \frac{\Omega_{\text{DE},0}}{\Omega_1}. \quad (1.7)$$



H. Cheng et al. arXiv:2505.02932

Including terms up to second order in (1.1), and defining

$$\Omega_2 \equiv \frac{3}{4} \frac{p_2}{\rho_{\text{crit}}}, \quad (1.8)$$

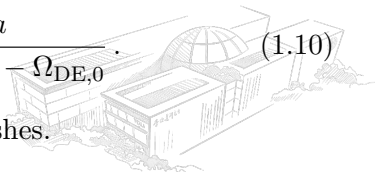
the DE density becomes:

$$\rho(a) = \rho_{\text{DE},0} \left[1 + (a-1) \left(\frac{\Omega_1 + \Omega_2}{\Omega_{\text{DE},0}} \right) + \frac{2}{5} (1-a^2) \frac{\Omega_2}{\Omega_{\text{DE},0}} \right]. \quad (1.9)$$

The equation-of-state parameter is then:

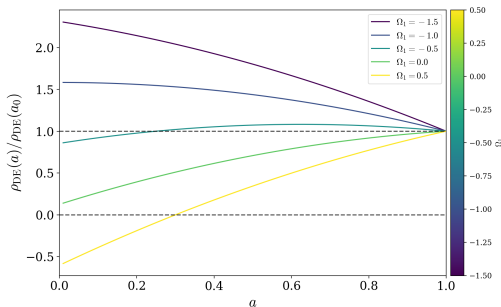
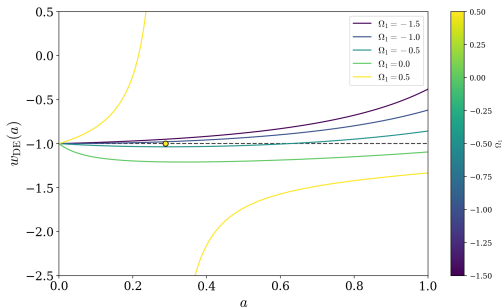
$$w_{\text{DE}}(a) = -1 + \frac{1}{3} \frac{(\Omega_1 + (1 - \frac{4}{5}a)\Omega_2)a}{\left[\Omega_1 + \frac{3}{5}(1 - \frac{2}{3}a)\Omega_2 \right] (1-a) - \Omega_{\text{DE},0}}. \quad (1.10)$$

This expression can exhibit poles when the denominator vanishes.



Fixing $\Omega_2 = 1$ and $\Omega_{\text{DE},0} = 0.7$ while varying Ω_1 , the model can reproduce:

- ▶ Quintessence behavior ($-1 < w_{\text{DE}} < -\frac{1}{3}$),
- ▶ Phantom DE ($w_{\text{DE}} < -1$),
- ▶ Phantom crossing (w_{DE} crosses -1), and
- ▶ Poles in w_{DE} where ρ_{DE} changes sign.

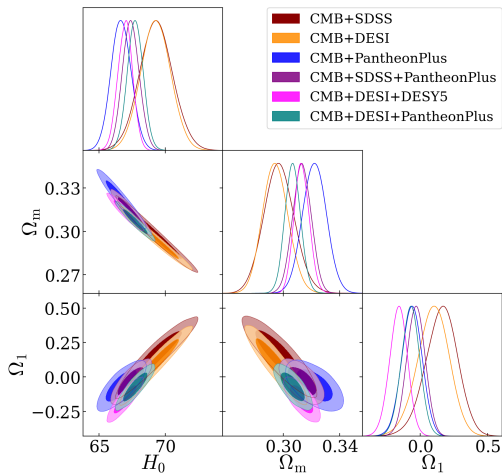


H. Cheng et al. arXiv:2505.02932

Dataset	Ω_1	H_0	Ω_m	$\Delta\chi^2_{\Lambda\text{CDM}}$
CMB only	$0.89^{+0.62}_{-0.14}$	83^{+10}_{-7}	$0.217^{+0.019}_{-0.074}$	-4.13
CMB+SDSS	$0.16^{+0.12}_{-0.11}$	69.3 ± 1.3	0.297 ± 0.011	0.23
CMB+DESI	$0.095^{+0.12}_{-0.11}$	69.3 ± 1.1	0.2946 ± 0.0090	0.7
CMB+PP	-0.062 ± 0.075	66.68 ± 0.76	0.3221 ± 0.0084	0.34
CMB+SDSS+PP	-0.032 ± 0.068	67.40 ± 0.64	0.3132 ± 0.0065	0.28
CMB+DESI+DESY5	-0.162 ± 0.067	66.98 ± 0.56	0.3131 ± 0.0053	-7.35
CMB+DESI+PP	-0.072 ± 0.068	67.74 ± 0.61	0.3068 ± 0.0056	-0.33

Key Findings

- ▶ CMB+SDSS, CMB+DESI trend in the right direction to alleviate H_0 and S_8 tensions
- ▶ CMB+DESI+DESY5 shows $> 2\sigma$ deviation from ΛCDM
- ▶ Other cosmological parameters remain close to Planck ΛCDM values



H. Cheng et al. arXiv:2505.02932

► CMB+DESI:

$$H_0 = 69.3 \pm 1.1 \text{ km/s/Mpc}$$

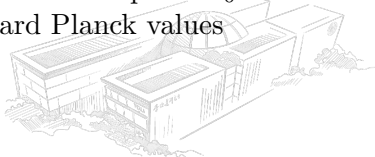
$$\Omega_m = 0.2946 \pm 0.0090 ;$$

CMB+PP:

$$H_0 = 66.68 \pm 0.76 \text{ km/s/Mpc}$$

$$\Omega_m = 0.3221 \pm 0.0084$$

- Adding SNe data pulls H_0 and Ω_m toward Planck values



Second-Order Expansion Results



Dataset	Ω_1	Ω_2	$\Delta\chi^2_{\Lambda\text{CDM}}$
CMB	$0.42^{+1.1}_{-0.83}$	> -0.0245	-5.34
CMB+SDSS	$-0.64^{+0.41}_{-0.86}$	> 1.23	-1.81
CMB+DESI	$-1.25^{+0.21}_{-0.53}$	> 2.69	-6.46
CMB+PP	$-0.52^{+0.39}_{-0.65}$	$1.4^{+2.0}_{-1.1}$	-0.93
CMB+SDSS+PP	-0.72 ± 0.33	1.96 ± 0.92	-3.92
CMB+DESI+DESY5	$-1.21^{+0.19}_{-0.31}$	$2.94^{+1.0}_{-0.31}$	-19.24
CMB+DESI+PP	-0.84 ± 0.29	2.15 ± 0.80	-6.36

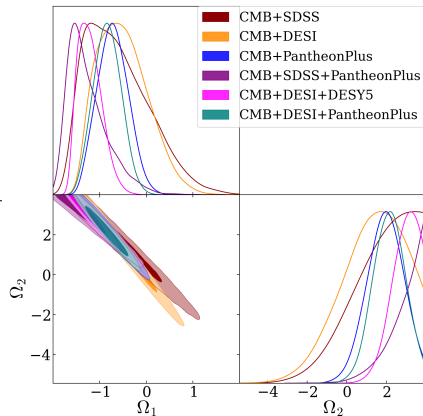
Strongest Evidence

CMB+DESI+DESY5:

- ▶ 4σ preference over ΛCDM
- ▶ Bayesian factor $\Delta \ln \mathcal{Z} = 3.67$

Key Features

- ▶ Strong negative correlation between Ω_1 and Ω_2 .



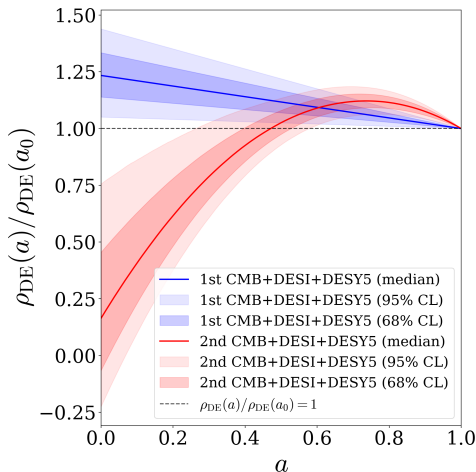
H. Cheng et al. arXiv:2505.02932

First-Order Model:

- ▶ Mild evolution
- ▶ $\rho_{DE}(a)/\rho_{DE,0}$ stays near unity
- ▶ Narrow confidence intervals

Second-Order Model:

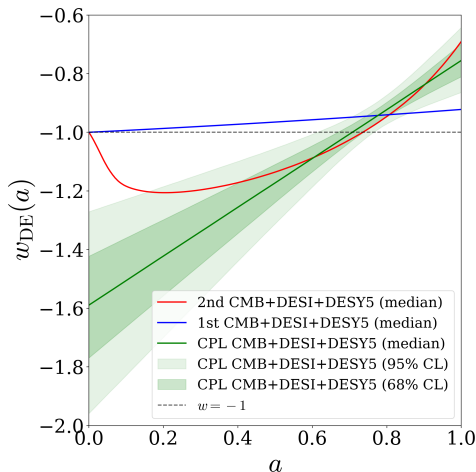
- ▶ Deviate Λ CDM CC (Largest CMB+DESI+DESY5 more than 2σ)
- ▶ Non-monotonic behavior
- ▶ Peak at $a \approx 0.7 - 0.8$ ($z \approx 0.3 - 0.4$)



H. Cheng et al. arXiv:2505.02932

Key Features:

- ▶ First-order: Stays in quintessence regime
- ▶ Second-order: Crosses phantom divide ($w_{\text{DE}} = -1$) at $a \approx 0.7 - 0.8$ ($z \approx 0.3 - 0.4$)
- ▶ Agreement with CPL at late times



H. Cheng et al. arXiv:2505.02932

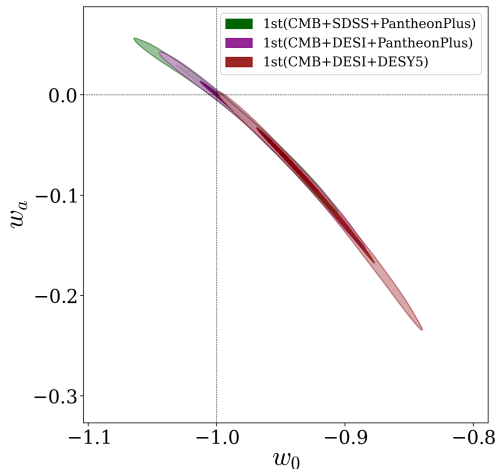
Present-day EoS:

$$w_0 \equiv w_{DE}(a = 1)$$

$$w_a \equiv - \left. \frac{dw_{DE}}{da} \right|_{a=1}$$

First-Order:

- ▶ Tight constraints
- ▶ Near Λ CDM point
- ▶ Strong w_0 - w_a degeneracy



H. Cheng et al. arXiv:2505.02932

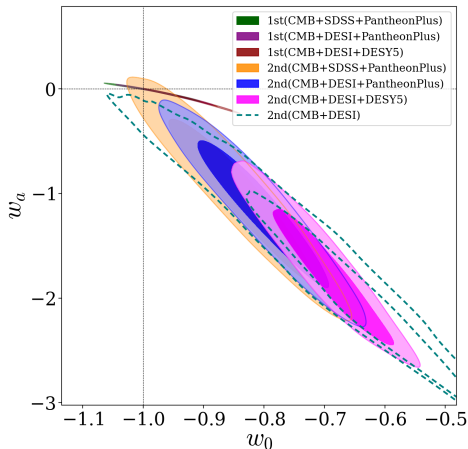
Second-Order:

- ▶ $w_0 > -1$ (quintessence today)
- ▶ $w_a < 0$ (evolution toward phantom)
- ▶ CMB+DESI+DESY5: $> 2\sigma$ from Λ CDM

Dataset Comparison

DESI \rightarrow stronger DDE preference than SDSS

DESY5 \rightarrow stronger DDE preference than PP



H. Cheng et al. arXiv:2505.02932

First Order Model

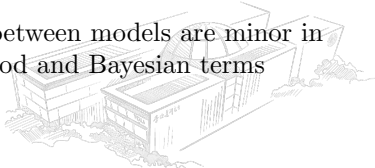
Dataset	$\Delta\chi_{\min, \text{CPL}}^2$	$\Delta \ln \mathcal{Z}_{\text{CPL}}$
CMB	0.96	0.55
CMB+SDSS	2.68	1.21
CMB+PP	1.85	2.05
CMB+SDSS+PP	4.45	0.93
CMB+DESI	8.25	-1.94
CMB+DESI+DESY5	12.1	-2.71
CMB+DESI+PP	7.2	-0.1

- ▶ All $\Delta\chi^2$ values are worse than CPL
- ▶ Datasets without DESI show positive $\Delta \ln \mathcal{Z}$ (better than CPL due to 1 less parameter)

Second Order Model

Dataset	$\Delta\chi_{\min, \text{CPL}}^2$	$\Delta \ln \mathcal{Z}_{\text{CPL}}$
CMB	-0.25	-0.26
CMB+SDSS	0.64	0.53
CMB+PP	0.57	1.02
CMB+SDSS+PP	0.26	0.78
CMB+DESI	1.09	-0.89
CMB+DESI+DESY5	0.21	0.96
CMB+DESI+PP	1.18	0.6

- ▶ All $|\Delta\chi^2|$ and $|\Delta \ln \mathcal{Z}|$ values < 1
- ▶ Differences between models are minor in both likelihood and Bayesian terms



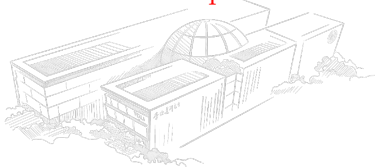
① First-Order Model:

- ▶ Generally consistent with Λ CDM
- ▶ CMB+SDSS, CMB+DESI alleviate H_0 and S_8 tensions

② Second-Order Model:

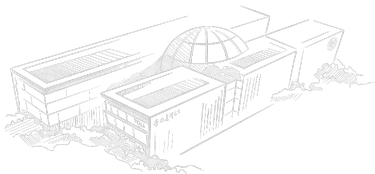
- ▶ Distinctive non-monotonic behavior in both energy density and $w_{\text{DE}}(a)$ evolution
- ▶ Late time $w_{\text{DE}}(a)$ shows strong agreement with the CPL parameterization across datasets (Phantom crossing behavior and Dark energy is weakening)

- ③ CMB+DESI+DESY5 always give much stronger preference for DDE compared to other datasets combination.

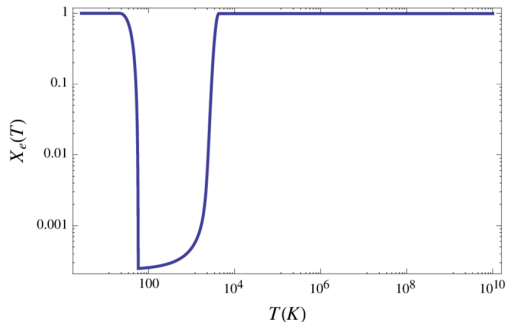




- 1 Constraining Pressure-Based Dynamical Dark Energy(DDE) Models with Latest Cosmological Data
- 2 **Constraining exotic high- z reionization histories with Gaussian processes and the cosmic microwave background**



- ▶ Intergalactic gas transitioned from cold and neutral to hot and ionized
- ▶ Complex mechanisms: structure formation, thermodynamics, astrophysical sources

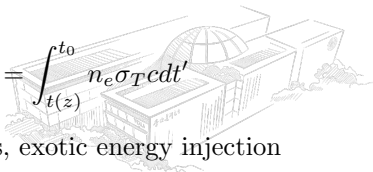


CMB Signatures

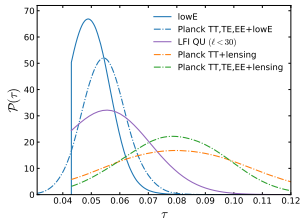
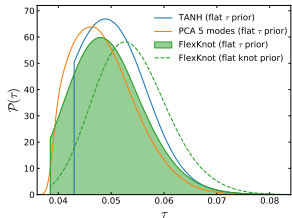
- 1 Temperature Anisotropies
- 2 Polarization
- 3 kSZ (kinetic Sunyaev-Zel'dovich) effect

Key quantity: electron Thomson scattering optical depth

$$\tau(z) = \int_{t(z)}^{t_0} n_e \sigma_T c dt'$$



New Physics Sources: Dark matter decay, primordial black holes, exotic energy injection



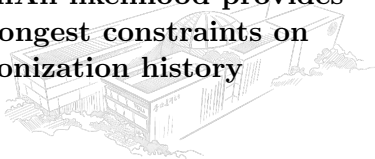
Planck 2018 results (arxiv:1807.06209)

Planck 2018 Results:

- ▶ $\tau = 0.0519^{+0.0030}_{-0.0079}$
(lowE; flat prior; TANH)

Key Points:

- ▶ Large-scale polarization tightens constraints
- ▶ Planck low- ℓ EE-only SimAll likelihood provides strongest constraints on reionization history



▶ Innovation:

- ▶ Implement a new, flexible **Gaussian Process (GP)-based reionization scheme**, called `reio_gpr_tanh`, in the CLASS code.
- ▶ Constrain **high-redshift reionization** histories using GP-based reionization scheme and CMB data.
- ▶ First propose use **high-redshift optical depth, $\tau_{\text{high}z}$ posterior** to constrain energy ejection in reionization history.

▶ Advantages:

- ▶ Model-independent reconstruction of $X_e(z)$
- ▶ The $\tau_{\text{high}z}$, offers tighter constraints on new physics sources compared to the low-redshift optical depth $\tau_{\text{low}z}$.

▶ **Public Code:** https://github.com/Cheng-Hanyu/CLASS_reio_gpr

▶ **Dataset:** Analysis with Planck 2018 low- ℓ EE likelihood



RBF Kernel:

$$k(z_1, z_2) = \sigma_f^2 \exp \left[-\frac{(z_1 - z_2)^2}{2l^2} \right] \quad (2.1)$$

GP Prediction:

$$X_e^{\text{GP}}(z) = \bar{m}(z) + \mathbf{k}_*^T \mathbf{K}^{-1} [\mathbf{X}_{\text{train}} - \bar{m}(\mathbf{z}_{\text{train}})] \quad (2.2)$$

Key Parameters:

- ▶ σ_f : Overall variance scale
- ▶ l : Correlation length in redshift space
- ▶ Training points: $\{(z_i, X_e^{\text{IN}}(z_i))\}$
- ▶ \mathbf{k}_* is the vector of covariances between the new point z and each training redshift z_i (i.e. $\mathbf{k}_{*,i} = k(z, z_i)$)
- ▶ \mathbf{K}^{-1} is the inverse matrix of the kernel function \mathbf{K} ($\mathbf{K}_{ij} = k(z_i, z_j)$)
- ▶ $\bar{m}(z) = 0$: mean function (Set = 0 in our case.)



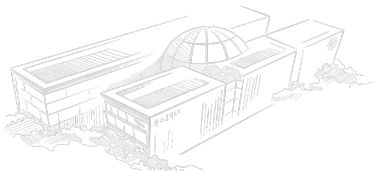
Adaptive binning: Smaller intervals at low- z , larger at high- z

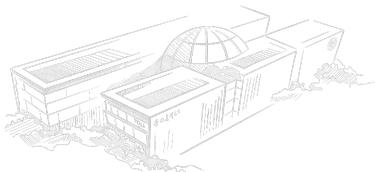
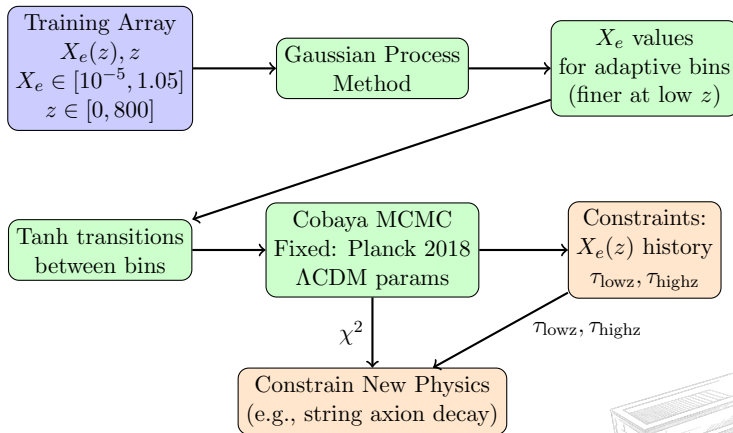
Tanh Transition Formula:

$$X_e(z) = X_e^{\text{GP}}(z_i) + \frac{1}{2} \left[1 + \tanh \left(\frac{z - z_{\text{jump}}}{\Delta z} \right) \right] \times [X_e^{\text{GP}}(z_{i+1}) - X_e^{\text{GP}}(z_i)] \quad (2.3)$$

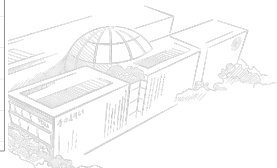
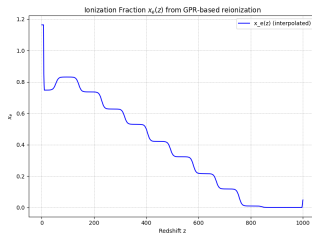
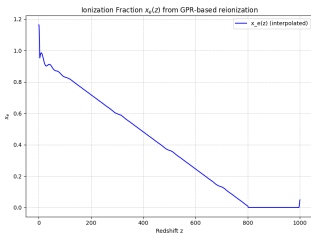
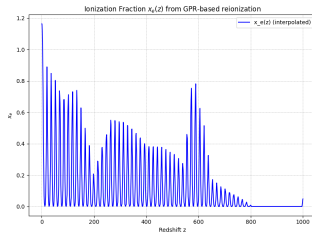
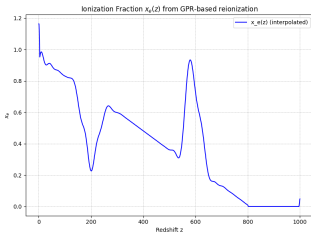
Boundary Conditions:

- ▶ Low- z (post-reionization): $X_e \approx 1 + \frac{Y_{\text{He}}}{4(1-Y_{\text{He}})}$
- ▶ High- z (pre-reionization): $X_e \approx 10^{-5}$

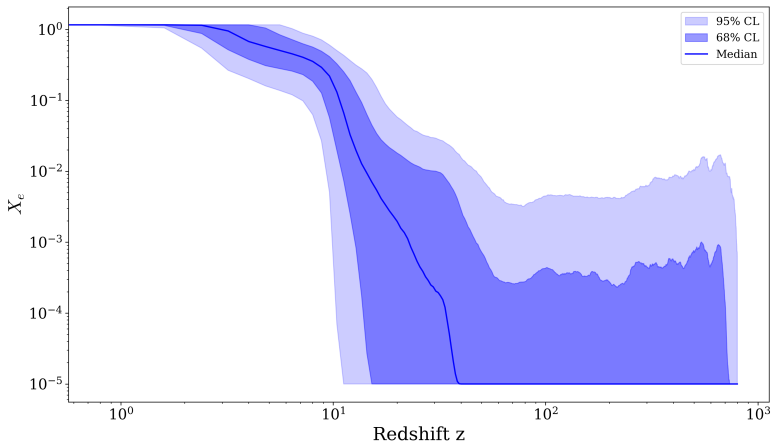




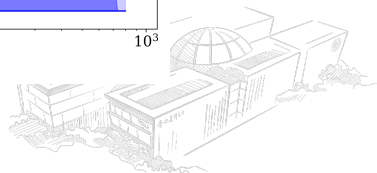
Demonstrate the flexibility of our method to explore the X_e - z parameter space.



Reconstruction history of $X_e(z)$



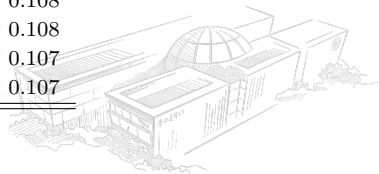
H. Cheng et al. arXiv:

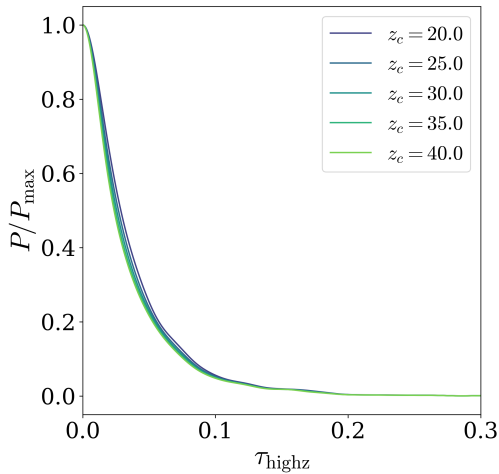
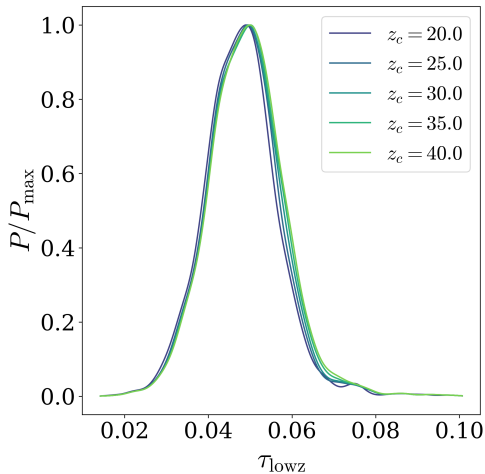


Parameter Definitions

- ▶ z_c : Critical redshift separating low and high redshift regimes
- ▶ $\tau_{\text{low}z}$: Optical depth integration for $z \in [0, z_c]$
- ▶ $\tau_{\text{high}z}$: Optical depth integration for $z \in [z_c, z_{\text{max}}]$ ($z_{\text{max}} = 800$ set by hand)

z_c	68% CL		95% CL	
	$\tau_{\text{low}z}$	$\tau_{\text{high}z}$	$\tau_{\text{low}z}$	$\tau_{\text{high}z}$
20.0	$0.0474^{+0.0079}_{-0.0080}$	< 0.036	$0.047^{+0.018}_{-0.017}$	< 0.109
25.0	$0.0480^{+0.0080}_{-0.0080}$	< 0.035	$0.048^{+0.018}_{-0.017}$	< 0.108
30.0	$0.0483^{+0.0083}_{-0.0080}$	< 0.035	$0.048^{+0.018}_{-0.017}$	< 0.108
35.0	$0.0486^{+0.0086}_{-0.0081}$	< 0.035	$0.049^{+0.018}_{-0.017}$	< 0.107
40.0	$0.0488^{+0.0088}_{-0.0082}$	< 0.035	$0.049^{+0.019}_{-0.017}$	< 0.107

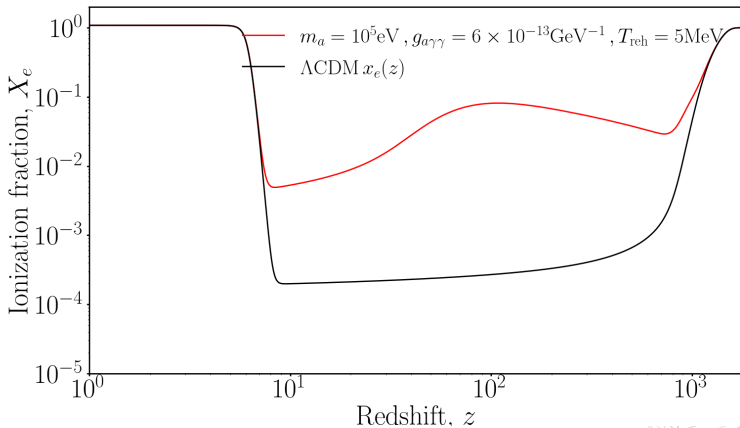




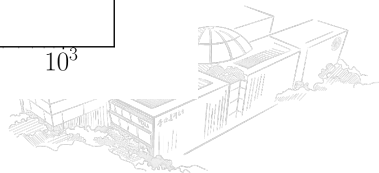
H. Cheng et al. arXiv:

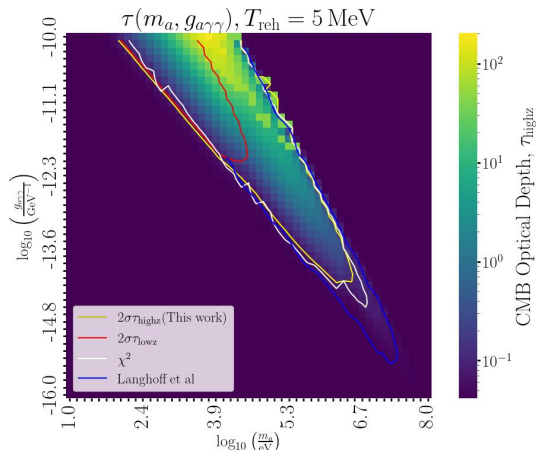


Example for “irreducible” axion decay



H. Cheng et al. arXiv:





H. Cheng et al. arXiv:

95% CL upper limits:

- ▶ $\chi^2 < 403.2$
- ▶ $\tau_{\text{highz}} < 0.111$

Key Finding:

- ▶ τ_{highz} statistics provide constraints comparable to those from Langhoff et al. (arXiv:2209.06216), who derived constraints from freeze-in abundance.
- ▶ τ_{highz} statistics and χ^2 analyses agree well,
- ▶ τ_{highz} providing conservative constraints compared to χ^2 analyses using Planck low- ℓ EE-only likelihood. (reliable)

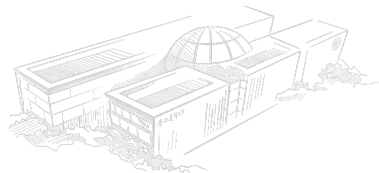
- ▶ **Model-independent approach:** Used GP method to sample random reionization histories $X_e(z)$
 - MCMC analysis with $\mathcal{O}(20)$ GP parameters
 - Planck low- ℓ EE-only SimAll likelihood
- ▶ **New derived parameter:** $\tau_{\text{high}z}$ - high- z contribution to CMB optical depth
 - Extended existing Planck analyses to high- z
 - Verified via χ^2 analysis to be reliable
 - Model-independent posterior for testing any energy injection model
- ▶ **Applications:**
 - Decaying “irreducible” axion DM constraints
 - String axion constraints (See Ziwen Yin’s poster)
- ▶ **Importance:** Offer a clean and general way to constrain new physics using $\tau_{\text{high}z}$ posterior.
- ▶ **Public Code:** https://github.com/Cheng-Hanyu/CLASS_reio_gpr
<https://github.com/ZiwenYin/Reionization-with-multi-axions-decay>

Thanks



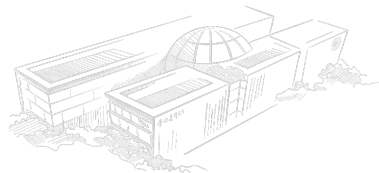
李政道研究所
TSUNG-DAO LEE INSTITUTE

Thanks





Questions?



First Order ($\Omega_2 = 0$): Dark energy = cosmological constant + fluid with $w = -4/3$ (phantom)

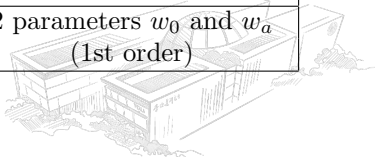
$$\rho = \rho_{\text{DE},0} \left[\left(1 - \frac{\Omega_1}{\Omega_{\text{DE},0}} \right) + \frac{\Omega_1}{\Omega_{\text{DE},0}} a \right] \quad (4.1)$$

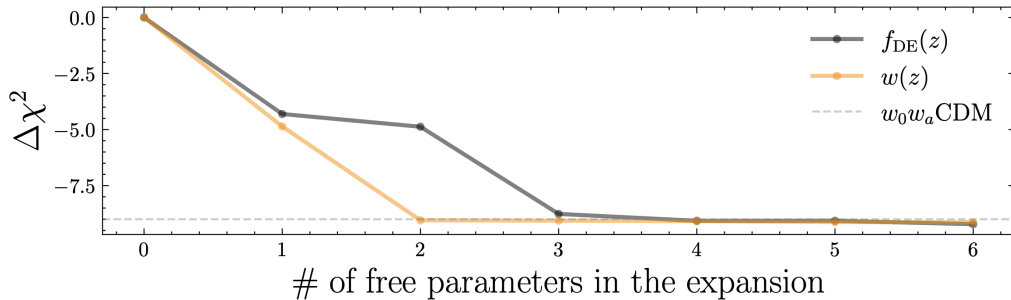
Second Order: Dark energy = cosmological constant + two fluids ($w = -4/3$ and $w = -5/3$)

$$\rho = \rho_{\text{DE},0} \left[\left(1 - \frac{\Omega_1}{\Omega_{\text{DE},0}} - \frac{3}{5} \frac{\Omega_2}{\Omega_{\text{DE},0}} \right) + \left(\frac{\Omega_1}{\Omega_{\text{DE},0}} + \frac{\Omega_2}{\Omega_{\text{DE},0}} \right) a - \frac{2}{5} \frac{\Omega_2}{\Omega_{\text{DE},0}} a^2 \right] \quad (4.2)$$

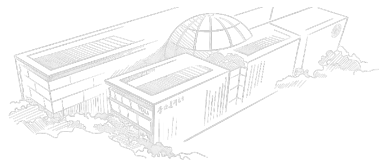
	Pressure Parameterization	CPL Parameterization
$a = 0$	$w = -1$	$w = w_0 + w_a$
$a = \infty$	$w = -4/3$ (1st order), $w = -5/3$ (2nd order)	$w = \infty$
Parameters	1 parameter Ω_1 (1st order) 2 parameters Ω_1 and Ω_2 (2nd order)	2 parameters w_0 and w_a (1st order)

Not nested with CPL

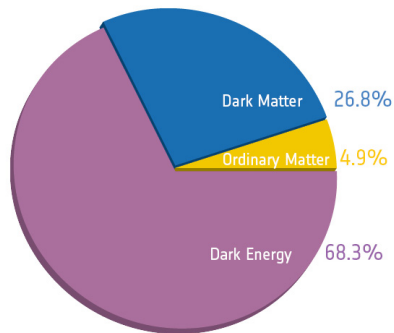




Planck 2018 results (arxiv:1807.06209)



- ▶ Universe's expansion is **accelerating**
- ▶ First evidence: Type Ia Supernovae (1998)
- ▶ **2011 Nobel Prize:** Saul Perlmutter, Brian Schmidt, Adam Riess
- ▶ Dark Energy (DE) $\approx 70\%$ of universe
- ▶ Standard model: Λ CDM
 - ▶ Λ = cosmological constant
 - ▶ CDM = Cold Dark Matter
- ▶ Recent challenges from DESI & DES



Key Features:

- ▶ Snapshot at $z \sim 1100$
- ▶ Temperature anisotropies
 $\Delta T/T \sim 10^{-5}$
- ▶ Acoustic peaks encode cosmology

Datasets Used:

- ▶ **Planck 2018:**
 - ▶ high- ℓ Plik TT, TE, EE likelihoods
 - ▶ low- ℓ TT-only Commander likelihood
 - ▶ low- ℓ EE-only SimAll
- ▶ **ACT DR6:** Lensing (actplanck baseline)
- ▶ Combined as "CMB"

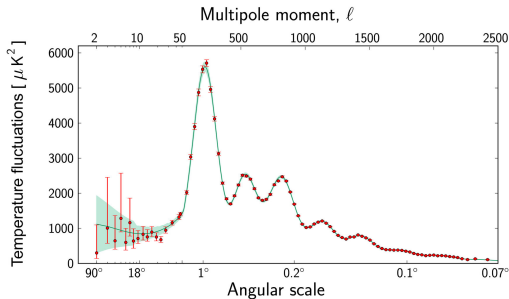


Figure 3: This graph shows the temperature fluctuations in the CMB detected by Planck at different angular scales on the sky from ESA and the Planck Collaboration.

Standard Ruler:

- ▶ Sound waves in early universe
- ▶ Frozen at recombination
- ▶ Characteristic scale ~ 150 Mpc
- ▶ Geometric Probe: Measures $D_A(z)$ and $H(z)$ directly through angular and radial BAO scales

Datasets:

- ▶ **SDSS**: the completed SDSS-IV eBOSS survey
- ▶ **DESI DR2**: 3-year data
- ▶ Redshift range: $0.1 < z < 4$

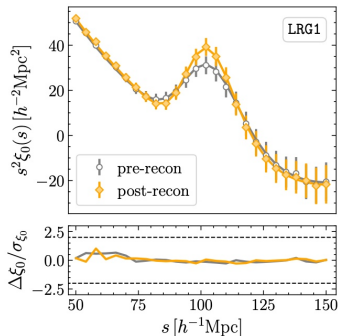


Figure 4: Two point correlation function of the average of 25 Abacus galaxy mock catalogs (data points) compared to the model prediction (lines) pre- (grey) and post-reconstruction (yellow) from DESI Collaboration.

Standard Candles:

- ▶ Uniform peak luminosity
- ▶ Distance ladder calibration
- ▶ Direct evidence for acceleration
- ▶ Late-time Probe: Directly measures luminosity distance $D_L(z)$ and expansion history

Datasets:

- ▶ **PantheonPlus:** 1550 SNe
 - ▶ $0.001 < z < 2.26$
- ▶ **DES Y5:** 1635 SNe
 - ▶ $0.1 < z < 1.13$

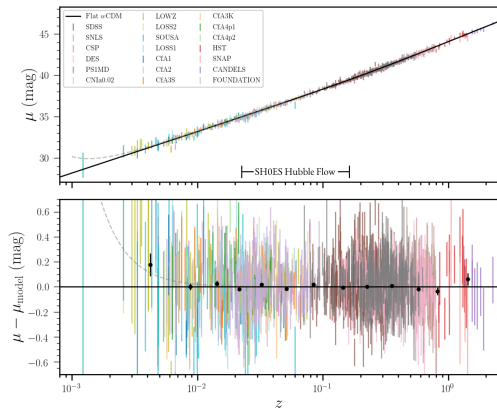


Figure 5: distance modulus vs redshift from The Pantheon+ Analysis paper (<https://arxiv.org/abs/2202.04077>)